Thin Solid Films 519 (2011) 3931–3938

Contents lists available at ScienceDirect

Thin Solid Films

journal homepage: www.elsevier.com/locate/tsf

# Poly(methyl methacrylate) nanocomposites based on $TiO_2$ nanocrystals: Tailoring material properties towards sensing

A. Convertino [a], M. Tamborra [b], M. Striccoli [b], G. Leo [a], A. Agostiano [b,c], M.L. Curri [b,*]

[a] ISMN-CNR Istituto per lo Studio dei Materiali Nanostrutturati, Via Salaria km. 29.300, 00016 Roma, Italy
[b] IPCF-CNR Istituto per i Processi Chimici e Fisici, Bari Division, Via Orabona 4, 70126 Bari, Italy
[c] Dipartimento di Chimica., Università di Bari, Via Orabona 4, 70126 Bari, Italy

ARTICLE INFO

*Article history:*
Received 29 June 2010
Received in revised form 24 January 2011
Accepted 25 January 2011
Available online 3 February 2011

*Keywords:*
Poly(methyl metacrylate)
Nanocomposite
Titanium dioxide
Surface chemistry
Chemical sensors

ABSTRACT

Nanocomposite materials have been obtained by dispersing organic capped $TiO_2$ nanocrystals (NCs) with different shape and surface chemistry in poly(methyl methacrylate) (PMMA) as a host medium. Films of the prepared nanocomposites based on $TiO_2$ NCs have been fabricated by spin coating and morphologically characterized as a function of the preparative conditions. The organic vapor absorption ability of the PMMA/$TiO_2$ NC based nanocomposites has been then investigated both for spherical and rod-like NCs, and the chemical nature of the coordinating organic molecules has been also varied. The results of the investigation have demonstrated that NC geometry and surface chemistry can modulate the specific absorption characteristics of the modified PMMA in order to absorb different solvent molecules (i.e. acetone, ethanol, propan-2-ol and water). Such features, due to specific interactions between the potential analyte vapors and the functionalized surface of NCs, can effectively be addressed in a controlled and reproducible way, thus offering original opportunities for designing innovative chemical sensors.



## 1. Introduction

Polymer nanocomposites consisting of oxide nanocrystals (NCs) embedded in organic polymer as a host medium are able to combine the peculiar characteristics of both organic and inorganic moieties in original functional materials. Such hybrid materials join peculiar characteristics of polymers, such as structural flexibility, convenient processability, and high thermal and mechanical stability with specific size dependent properties of inorganic nanocrystalline oxides, thus providing unique functions. Such cooperative combination of individual characteristics of each component offers excellent opportunities to fabricate unique materials with properties addressable in many application fields, including light-emitting diodes, optical switches, waveguides, transparent coatings and sensors [1–7].

The fabrication of such class of nanocomposites can be accomplished by dispersing the inorganic nanofillers in host polymer and generally two routes can be followed: i) "in situ" synthesis of nanoparticles in the polymer matrix [8,9] or, alternatively, reaction of polymer precursor in the presence of inorganic nanoparticles [10,11] and ii) "ex situ" incorporation of synthesized nanoparticles in organic polymers by exploiting a common solvent [12,13]. The former may produce undesired species in the host matrix, coming either from the products of the nanoparticle synthesis process or from the polymerization steps [14]. In addition a poor control on NC size and properties is a possible drawback of such approach. The mixing of synthesized inorganic NCs with selected polymers results in extreme benefits, since it allows for full control of both the inorganic and organic moieties. In this way, a possible formation of NC aggregates can be avoided, which may represent a limit of this approach.

In this perspective the use of chemical route enabling the synthesis of colloidal oxide NCs with excellent solubility in variety of solvents can allow the uniform dispersion of the nanofillers in the host matrix by playing with the direct interaction between the polymer and organic molecules coordinating the NC surface. Such molecules can derive directly from the NC synthesis or be introduced in a post-synthesis ligand exchange process to improve the compatibility with the polymer and/or to modify the characteristics of the composite [15].

The polymer based nanocomposites represent excellent candidates for many application oriented fields. In particular recent studies have reported that the ability of a polymer to absorb solvent molecules can be modified by filling the polymer with inorganic nanoparticles [16–23].

Polymer based networks upon exposure to solvent vapors can absorb the organic molecules and swell until an equilibrium state is reached. The tendency to absorb molecules is effectively compensated by the elastic characteristics of the material. In this scenario the ability to tune the gas or vapor diffusion into a polymer material in order to

* Corresponding author. Tel.: +39 080 5442027; fax: +39 080 5442128.
*E-mail addresses:* annalisa.convertino@ismn.cnr.it (A. Convertino), m.tamborra@ba.ipcf.cnr.it (M. Tamborra), m.striccoli@ba.ipcf.cnr.it (M. Striccoli), gabriella.leo@ismn.cnr.it (G. Leo), a.agostiano@ba.ipcf.cnr.it (A. Agostiano), lucia.curri@ba.ipcf.cnr.it (M.L. Curri).

0040-6090/$ – see front matter © 2011 Elsevier B.V. All rights reserved.
doi:10.1016/j.tsf.2011.01.359

achieve specific sensing properties would have a remarkable technological impact.

In nanocomposite materials the interaction between the active sites at nanoparticle surface and the polymer chains can play a crucial role on the selectivity, rate and efficiency of the absorption capability of the host polymer, thus enabling an accurate control on the swelling/shrinking behavior in the polymer composite.

In this perspective, nanoparticles offer outstanding advantages due to their high surface-to-volume ratio, which can dramatically increase the number of active sites available for interaction with analyte molecules. Furthermore the use of colloidal NCs as nanofillers would further benefit from the possibility of achieving nano-objects with a precise control on the size, shape and chemical characteristics of the surface, as well as by their prompt processability. Through their specific functionalization, colloidal NCs can effectively and selectively interact with different analytes.

In this work $TiO_2$ was selected as an active sensing material due to its high refractive index and wide energy gap, which can be further tuned when such a semiconductor is prepared at the nanoscale. Such nanosized semiconductor is able to add original optical properties to the host polymer, as also recently demonstrated in reports on sensing of $TiO_2$ thin films towards humidity, oxygen and organic vapors [24].

Here, $TiO_2$ colloidal NCs have been obtained by means of a chemical route which allows, by simply controlling the NC growth kinetics, to dictate the particle geometry, spherical or rod shaped. This synthetic strategy provide gram-scale quantities of NCs capped by oleic acid (OLEA) and dispersed in a chloroform solution [25]. Such nanofillers have been dispersed in poly(methyl methacrylate) (PMMA) by using a common solvent. In addition $TiO_2$ nanorods (NRs) capped with different organic coordinating molecules, namely dodecylphosphonic acid (DPA), obtained by a ligand exchange procedure, have been incorporated in PMMA in order to investigate the effect of the specific surface chemistry of NCs.

The obtained nanocomposites have been deposited as films by spin coating onto suitable substrates and characterized by transmission electron microscopy (TEM) analysis and atomic force microscopy (AFM) investigation to fully clarify the critical role played by the nanoscale shape and the organic capping of the fillers in the host polymer.

The swelling of the PMMA nanocomposite films has been investigated at room temperature by measuring vis-IR reflectance spectra of the samples deposited on Si substrates in the presence of solvent vapors. Different solvents, like acetone, ethanol, propan-2-ol and water, have been selected for their different polarity, different chain length, and their own ability for swelling pure PMMA.

The specific NC geometry, combined with their surface chemical properties has been demonstrated to affect the swelling behavior of the polymer. Such an issue has been investigated and discussed in order to evaluate the potential of such class of nanocomposites for sensing as well as for all the applications where the interaction between organic coated nanoparticles and analyte molecules plays a fundamental role.

## 2. Experimental details

All chemicals have been of the highest purity available and used as received without further purification or distillation. Titanium tetraisopropoxide ($Ti(OPr^i)_4$ or TTIP, 99.999%), trimethylamino-*N*-oxide dihydrate ($(CH_3)_3NO\cdot 2H_2O$ or TMAO, 98%), water solution) and oleic acid ($C_{18}H_{33}CO_2H$ or OLEA, 90%) have been purchased from Aldrich. All solvents have been of analytical grade and purchased from Aldrich.

Fourier Transform Infra Red (FT-IR) investigation has been performed by using a Perkin-Elmer Spectrum GX FT-IR System at room temperature on samples obtained directly from synthesis without any size sorting treatments.

Low resolution transmission electron microscopy (TEM) images have been recorded using a Jeol Tem 1011 microscope operating at an accelerating voltage of 100 kV.

Scanning atomic force microscopy (AFM) images of nanocomposite thin films have been recorded with a PSIA Xe-100 Scanning Probe Microscope, operating in non-contact mode.

UV–vis–NIR spectroscopical analysis has been carried out by using a Cary 5 spectrophotometer properly equipped for experiments in the presence of gas or vapor. In particular the samples could be inserted into a glass tube where a synthetic air (20.5% of $O_2$ in $N_2$) has been flowed as carrier gas at 200 sccm. Samples have been exposed to selected organic vapors introduced by bubbling synthetic air in vessels containing the correspondent organic liquids. A mass flow controller system has been operated by Omicron apparatus.

### 2.1. Synthesis of $TiO_2$ colloidal nanocrystals

Organic-capped anatase $TiO_2$ NCs have been synthesized by hydrolysis of titanium tetraisopropoxide (TTIP) using technical oleic acid (OLEA) as surfactant at low temperatures (80–100 °C), as reported elsewhere [25]. Hydrolysis of TTIP has been carried out by an excess of the aqueous base solution in the presence of TMAO as a catalyst for polycondensation. The morphology of the resulting $TiO_2$ NCs is thus modified by varying the rate of water supply in the reaction mixture. In particular spherical particles (about 6 nm size) have been obtained upon in-situ water release (from the slow esterification reaction of OLEA and added EG), while rod-like shaped NCs, (NRs) (30 nm of average length and 6 nm of diameter) have been guaranteed by direct injection of large aqueous base volume into a reagent mixture.

The extracted titania NCs (in the anatase form, as it comes out from the XRD profile in Ref. 25) can be dispersed in optically clear concentrated apolar solutions due to the OLEA surface coating, showing an excellent temporal stability.

### 2.2. Surface ligand exchange

The OLEA coating on $TiO_2$ NRs has been replaced with an alkylphosphonic acid by the following procedure. The as-prepared $TiO_2$ NRs have been repeatedly washed (at least 6 times) and a volume of 3–4 ml of $CHCl_3$ has been then added to the precipitate to prepare a turbid suspension. A dodecylphosphonic acid (DPA) 0.2 M solution in $CHCl_3$ has been subsequently dropped under stirring at room temperature until a clear solutions has been obtained. The resulting mixture has been allowed to stir at room temperature for 90 min, afterwards methanol has been added to re-precipitate the nanoparticles. The NCs have been then repeatedly washed and re-dispersed in $CHCl_3$, obtaining a transparent concentrated solution.

### 2.3. Nanocomposite preparation

Nanocomposites have been prepared by dispersing the different types of pre-synthesized $TiO_2$ NCs in PMMA by using chloroform as a common solvent. More precisely, 0.05 g of polymer powder have been added to chloroform solutions of the $TiO_2$ NCs at different concentrations (from 0.025 M to 0.2 M), obtaining nanoparticle loading in the polymer of 4 wt.%, 8 wt.%, 16 wt.% and 32 wt.%.

The mixtures have been gently stirred until complete dissolution of the polymer in the solvent. Thin films have been obtained by spin-coating (by using an EC101DT Photo Resist Spinners, Headway Research Inc.) depositing few drops of the NC–polymer composites onto properly cleaned glass and silicon substrates at 3000 rpm for 30 s. A thermal treatment at 60 °C for 5 min has been then performed on the nanocomposite thin film to remove residual solvent. The film thickness, measured by means of Alpha-Step 500 surface profiler, has

been found in the range from 400 nm up to 1 μm, strongly depending on the NC concentration and surface ligand compositions.

TEM experiments have been carried out by depositing on drop of a dilute composite solution onto carbon-coated 400 mesh copper grids and spin coating at 6000 rpm.

### 2.4. Swelling experiments

The swelling characteristics of the fabricated nanocomposite thin films have been studied at room temperature by measuring the visible and infrared reflectance spectra of the samples deposited on Si substrates and in the presence of defined solvent vapors, namely acetone, ethanol, propan-2-ol and water. The selection of the solvents has been carried out by taking into account the different polarity, different chain length as well as their own ability in swelling pure PMMA.

The absorption of solvent molecules induce an increase in film thickness and, accordingly a shift in the position of the maxima detected in the reflectance spectral pattern of the PMMA based films.

## 3. Results and discussion

Nanocomposites based on colloidal $TiO_2$ NCs dispersed in PMMA have been prepared and characterized by spectroscopic and morphological measurements. The effects of the NC shape (nanorod and nanosphere, respectively) and the surface chemistry of the inorganic moiety, capped with oleic and phosphonic acid respectively, have been investigated and evaluated in terms of the structure and morphology of the resulting materials and of the absorption properties of the corresponding films upon exposure to different solvents.

Fourier transform infrared (FT-IR) spectroscopy has been used to probe the chemical nature of the organic coating on the surface of the $TiO_2$ NCs, in order to get insight on the chemical status of NC surface and confirm the effective capping exchange at the $TiO_2$ NC surface. $TiO_2$ powders for FT-IR analysis have been prepared by repeatedly washing the extracted precipitate in order to remove physisorbed surfactant molecules, and then evaporating the residual solvent under vacuum at room temperature.

In Fig. 1 the typical IR spectra recorded in the region 3600–800 $cm^{-1}$ of the pure OLEA (1a) and OLEA capped $TiO_2$ NRs (1b) are reported and compared. In both cases the spectra show, above 2000 $cm^{-1}$, in the fingerprint region, the typical signals characteristic of the alkyl chain of the OLEA molecule. In addition, the spectrum of the OLEA capped $TiO_2$ NCs exhibit the two characteristic bands at 1520 and 1436 $cm^{-1}$, which can be ascribed to the $COO^-$ antisymmetric and symmetric stretching vibrations of carboxylate anions complexed with surface Ti centers. No clear evidence of the free C=O stretching band at around 1650–1720 $cm^{-1}$ (cf. 1775 $cm^{-1}$ for OLEA in the vapor phase) induce to exclude the presence of both un-ionized OLEA monomers and dimers [26,27] eventually having the C=O involved in H-bonding with a Ti–$OH^{2+}$ surface group. Similar spectrum has been obtained for the OLEA capped $TiO_2$ spherical NCs (data not reported).

Fig. 1 displays the IR spectra of pure DPA (1c) and DPA-coated $TiO_2$ NRs (1d), after surface modification procedure. The complexity of the spectrum and broad appearance of the peaks ascribable to the phosphonic group in the characteristic region (just below 1300 $cm^{-1}$) make their interpretation quite difficult. After the capping exchange procedure, the P=O stretching band at 1226 $cm^{-1}$ is not detected anymore, while P–O stretching peaks at 1074, 1010, and 950 $cm^{-1}$ appear to be broadened and shifted to lower wavenumbers with respect to pure DPA. This evidence can be accounted by the coordination of phosphonate headgroups to the titania surface, involving both tridentate and bidentate attachment [28,29] thus accounting for the strong affinity of phosphonic acids for the $TiO_2$ surface.

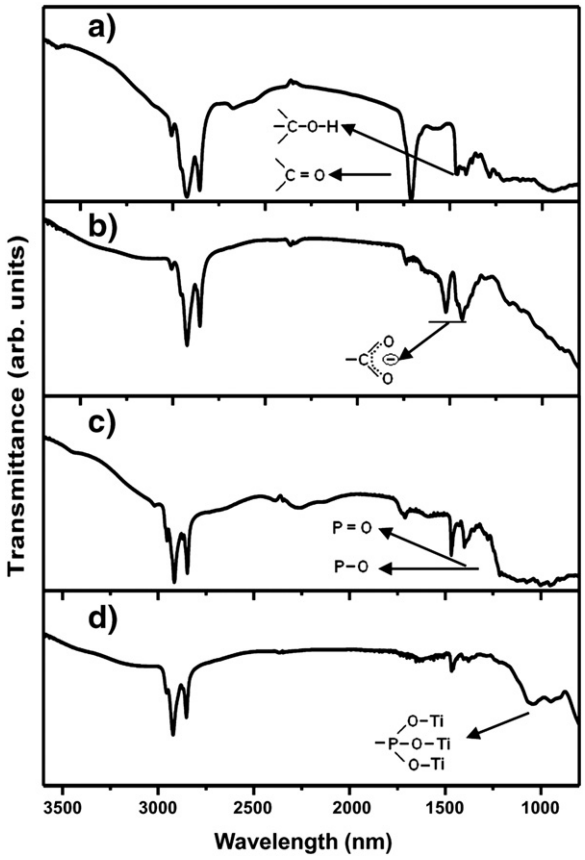


**Fig. 1.** FT-IR spectra of: (a) OLEA molecule; (b) OLEA capped $TiO_2$ NRs; (c) DPA molecule; and (d) DPA capped $TiO_2$ NRs.

The FT-IR analysis provides clear evidence of the carboxylate and phosphonic group, respectively from OLEA and DPA molecules, coordination to the NC surface atoms.

In Fig. 2 the TEM images of PMMA based nanocomposites incorporating OLEA and DPA capped $TiO_2$ NRs, respectively, are reported. The TEM pictures show, for both types of nanocomposites, the dispersion of NRs in the organic matrix. The occurrence of differently sized aggregates of NRs is evident, in spite of the fact that the NCs mantain their own individuality, preserving the original size achieved during the synthesis. It is relevant to point out that the extent of the dispersion of the nanofillers in the host polymer appears to be affected by the nature of the organic molecule coordinating the surface of $TiO_2$ NCs. In particular the NCs capped with phosphonic acid come out much more closely packed than the OLEA capped nanoparticles, once dispersed under the same condition in PMMA. Such a feature can be reasonably explained by the specific geometry of the two species, oleic acid and phosphonic acid, coordinating the NR surface, respectively. The former presents the aliphatic chain with a bend (due to the presence of a cis-double bond), while a linear geometry is characteristics for the latter (Scheme 1).

Accordingly a different packing extent is achievable for the two kinds of samples. Indeed only in the case of the phosphonic acid, linear chains can interdigitate and, thus, ensure a side-by-side arrangement of the $TiO_2$ NRs, that conversely, is not possible in the presence of OLEA capped NRs, which appear more dispersed and randomly arranged in the host polymer.

The surface morphology of nanocomposite films has been investigated as a function of the different NC shape and surface chemistry by AFM analysis.

Indeed in order to correlate the result of the AFM surface characterization with the structure of the bulk of the films, they were

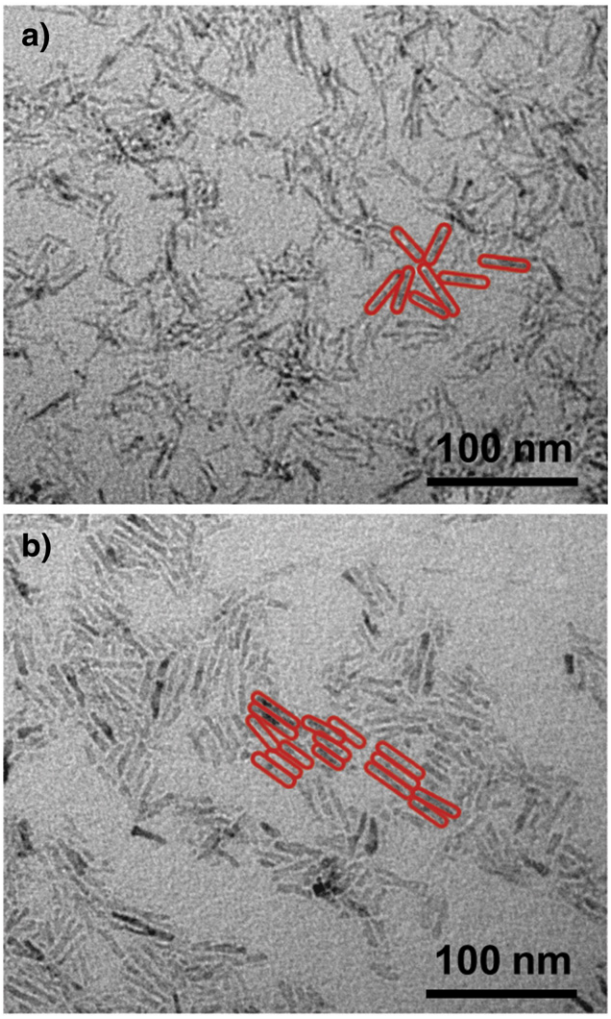


**Fig. 2.** TEM image of nanocomposite films formed by (a) OLEA capped and (b) DPA capped NRs dispersed in PMMA, respectively. The arrangement of the NRs in the two samples is highlighted in red.

combined with the insight deriving from TEM analysis, thus providing a complete picture of the nanocomposite characteristics.

Fig. 3 shows AFM plan view, recorded in non-contact mode, of OLEA and DPA capped $TiO_2$ NRs in PMMA, respectively. Two different nanoparticle loadings, namely 8 wt.% and 32 wt.%, have been considered. The AFM measurements have been performed on as-prepared samples and typically indicate a higher roughness of the $TiO_2$ NC based nanocomposite films with respect to the pure PMMA film (Rq = 0.3 nm, data not reported). The morphology is characterized by the presence of small and uniformly dispersed structures at the nanocomposite surface. Similar features have been observed for the composites based on OLEA capped spherical NCs in PMMA. The values of the root mean square roughness (RMS) for the NR modified PMMA films and average height of the detected structures (h) are reported in the caption of Fig. 3. In general, the lateral size of the objects imaged by the AFM is larger then the real dimension, due to the convolution effect of the tip, while the heights reflect the feature size more accurately [30]. Moreover, the average heights detected were referred to NC height protruding from the polymer thin film.

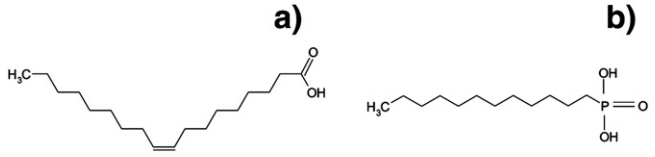


**Scheme 1.** Molecular structures of oleic acid (a) and dodecylphosphonic acid (b), respectively.

The roughness of $TiO_2$ based nanocomposites seems to be not influenced by NC loading, since no evidence of significantly different morphological feature, neither in terms of the size or number of structures at the polymer surface, is recorded as the concentration of $TiO_2$ NCs increases in the polymer. Only a slight enhancement (from about 1.4 nm to 2.0 nm) in the surface roughness of nanocomposite films can be observed moving from the OLEA capped $TiO_2$ NRs embedded in PMMA to the equivalent DPA capped NC based composites (Fig. 3c–d). Such feature is in a good agreement with the occurrence of larger aggregates ascribable to the formation of closely packed titania assemblies for the nanocomposites embedding DPA capped NRs, as demonstrated by TEM investigation (Fig. 2).

It is worth to observe that features compatible with the occurrence of porosity on the surface of the films are not present at low NC contents irrespectively of the organic capping.

Fig. 4 shows the measured solvent uptake, $\delta_\infty$, at the equilibrium, i. e. at time $t = \infty$, and the response rise time of the PMMA composites as a function of the $TiO_2$ NC loadings in the case of OLEA capped nanospheres and OLEA and DPA capped NRs for the four vapors tested, namely water, acetone, ethanol and propan-2-ol.

The solvent uptake $\delta t$ at time $t$, is defined as follows:

$$\delta t = (d_t - d_0) / d_0 * 100$$

being $d_0$, the initial thickness of the pristine film and $d_t$ that of the swollen sample at time $t$.

The values have been obtained by fitting the experimental reflectance spectra of the $TiO_2$ NC containing PMMA films deposited on Si substrates before and after a time of exposure, $t$, to solvent vapors. The standard matrix method [31] has been used to perform the numerical analysis of such spectra, using the optical constants measured on reference samples deposited onto the quartz substrate [20] to describe the theoretical curves, with the assumption that only a negligible variation of the refractive index of the PMMA nanocomposite is caused by the absorption of the solvent vapors [32].

Fig. 4a), b), c) and d) shows as a general trend an enhancement of solvent uptake in composites at lower $TiO_2$ loadings (≤8%wt.), when compared to pure PMMA (0%wt.). Only the PMMA composite containing $TiO_2$ NRs presents, upon exposure to the investigated polar solvents, water and acetone, a distinct behavior, since an immediate decrease in $\delta_\infty$ even at low loadings of $TiO_2$ is observed. Higher $TiO_2$ NC concentrations, either spherical or rod-like, induce a decrease in the $\delta_\infty$ values, as has been already observed in the literature for similar polymer composites [33–35]. Such behavior observed for NC loadings higher than 8%wt. can be reasonably ascribed to three distinct and concomitant effects: a) the net reduction of the polymer fraction in the nanocomposite composition, which is the active component of the hybrid system, that induces a lower absorption of solvent molecules, b) the increasing of the inorganic component, which somehow hinders the ability of polymer chains to arrange and thus to accommodate solvent molecules, c) a possible occurrence of nanofiller aggregation, with the consequent reduction of the sites available for the interaction with the penetrating molecules as it will be more in detail described in the following. In the case of DPA capped $TiO_2$ NRs an intermediate behavior between the OLEA capped nanosphere and NRs is observed. In particular, the response at low $TiO_2$ loadings seems enhanced in the presence of weakly polar solvents and slightly modified in the presence of the polar solvents by the inclusion of the DPA capped NRs.

Fig. 4e), f) g) and h) shows the response rise time of the PMMA composites as a function of the $TiO_2$ NC loadings in the case of OLEA capped nanospheres, and OLEA and DPA capped NRs respectively, for

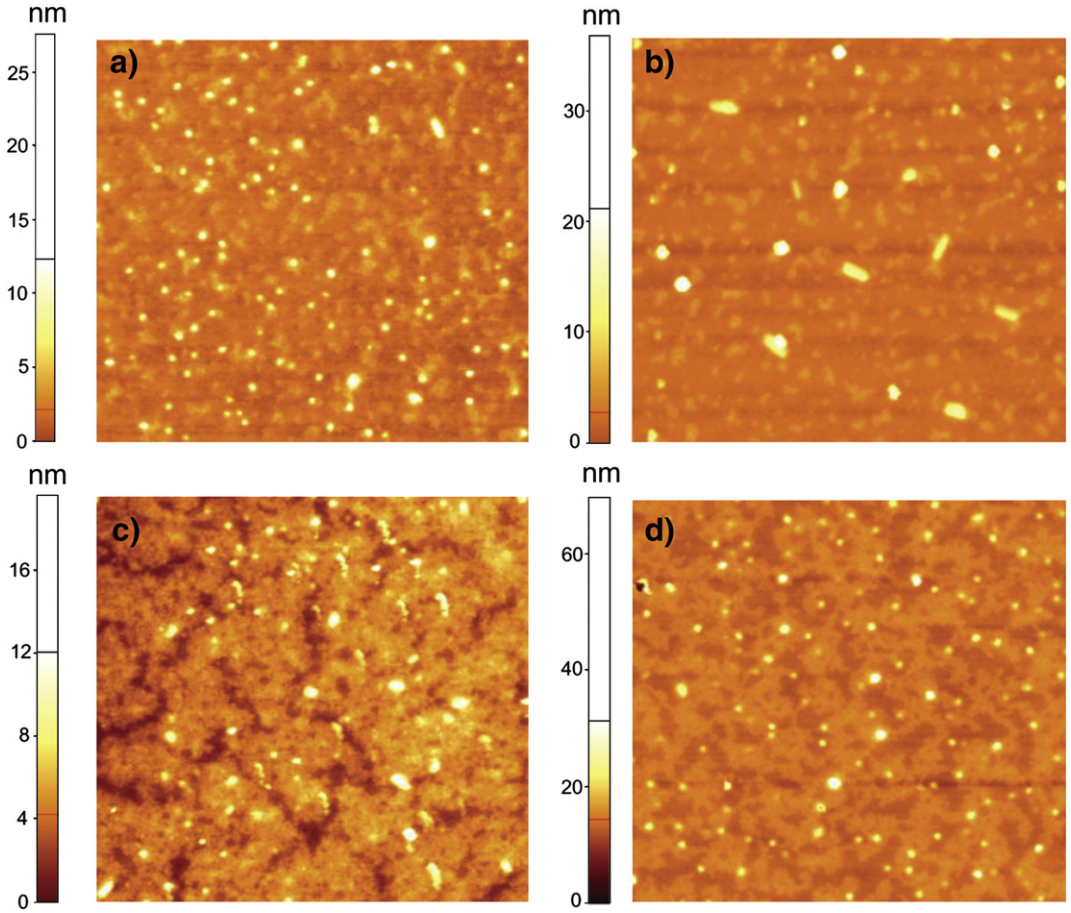


**Fig. 3.** AFM topographic images (3 μm × 3 μm scan size) recorded for PMMA based nanocomposites at different NR loading and surface chemistry: (a) 8 wt.% OLEA capped $TiO_2$ NRs (RMS = 1.4 nm; h = 12 nm); (b) 32 wt.% OLEA capped $TiO_2$ NRs (RMS = 1.5 nm; h = 12 nm); (c) 8 wt.% DPA capped $TiO_2$ NRs (RMS = 2.0 nm; h = 13 nm); and (d) 32 wt.% DPA capped $TiO_2$ NRs (RMS = 2.1 nm; h = 20 nm).

the four vapors tested. OLEA capped nanospheres seem to contribute to speed up the response of the PMMA composites when exposed to the polar solvents. Instead, the NRs, regardless of the chemical nature of the capping molecules, show a slower swelling response of the PMMA composite, with respect to the pure PMMA film, once exposed to polar solvents. In particular the OLEA capped NRs appear more effective in retarding the response of PMMA than the DPA capped counterparts. The presence of NCs in the PMMA speeds up the response of the PMMA composite when exposed to the weakly polar solvents. In particular, a relevant decrease of the rise time is observed in the PMMA filled by OLEA capped NRs in the presence of ethanol and propan-2-ol. It is relevant to remark that the presence of the NCs significantly alters the response of the PMMA towards a specific analyte, inducing modifications which are strongly dependent on the shape of the inorganic nanofillers and their specific surface chemistry. The variation in the NC geometry and in the chemistry of the molecules coordinating their surface can enhance or inhibit the swelling phenomena in the presence of organic molecules, as potential analytes, also varying the response time of the corresponding PMMA nanocomposites.

In order to focus the role of the shape and capping of the NC inclusions we plot in Fig. 5 the variation of the PMMA absorption capacity induced by the fillers in a more effective and quantitative way, by plotting the histogram of the relative variation of $\delta_\infty$, given in Fig. 4a), b), c) and d), for the PMMA nanocomposite films with respect to corresponding values obtained for the pure PMMA film, $\Delta\delta/\delta = (\delta_{TiO_2/PMMA} - \delta_{PMMA})/\delta_{PMMA}$. Such a variation has been reported as a function of the NC shape and nature of the capping molecules coordinating the NC surface for all the investigated solvent vapors, at a fixed NC content of 4%wt., being μ the electric dipole moment of the solvent molecule.

The overall indication is that films containing $TiO_2$ nanospheres provide an enhanced response to the polar solvents, acetone and water, when compared with the $TiO_2$ NR based counterparts, which in fact decrease the absorption capacity of the PMMA toward such type of solvents. The exposure to weakly polar solvents, such as ethanol and propan-2-ol, generally turns out in an increasing swelling in the nanocomposites, irrespective of the geometry of NCs, although a slightly higher response is observed for the NRs based nanocomposite. Remarkably, the PMMA nanocomposites upon exposure to propan-2-ol vapors, generally considered ineffective for swelling bare PMMA, report a significant increase in swelling. Such occurrence has been observed for the nanocomposite based on both rod-like and spherical types of NCs, and points out a dramatic change in the response of the composite materials towards propan-2-ol, when compared to the the bare PMMA. Hence, Fig. 5 unequivocally demonstrates that the presence of organic capped NCs at low loadings in the PMMA host matrix can influence the process of solvent absorption, either enhancing or reducing the response towards different solvent vapors, according to the specific characteristics of the nanofillers.

The AFM images confirm that, at low NC content, no change of film porosity as a function of the NC shape and capping can be detected, hence the different solvent uptakes measured cannot be accounted by such morphological feature.

The occurrence of void volume surrounding the $TiO_2$ NCs, as reported by Convertino et al. [18] is not sufficient alone to explain the observed phenomena. Indeed such voids should somehow enhance

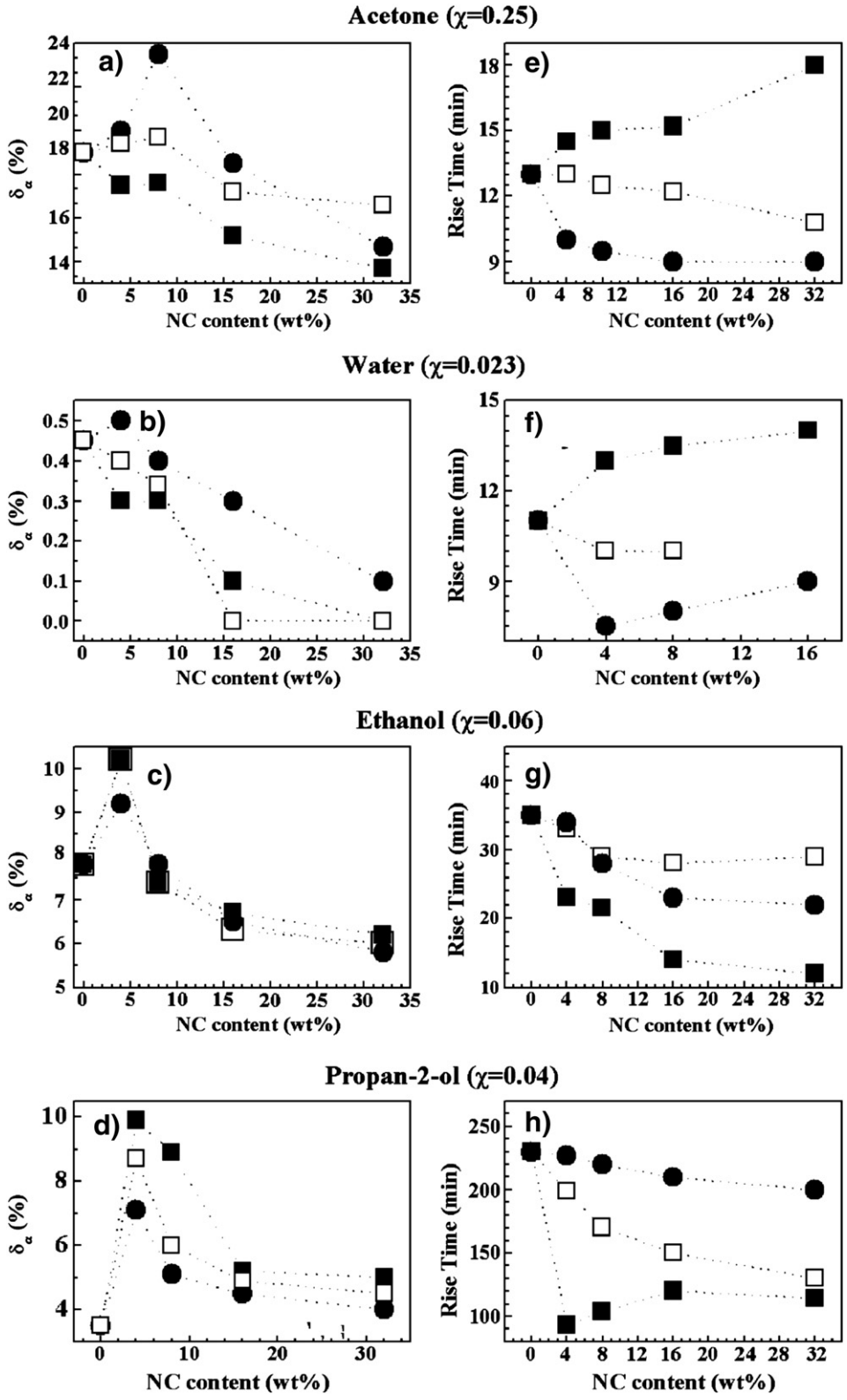


**Fig. 4.** Solvent uptake at the equilibrium, $\delta_\infty$, and the response rise time of the PMMA composite as a function of the $TiO_2$ loading in the case OLEA capped nanospheres (dot symbols), OLEA capped NRs (full square symbols), and DPA capped NRs (empty square symbols) for the exposure to vapors of acetone (Panel a) and e), respectively), water (Panel b) and f)), ethanol (Panel c) and g)), and propan-2-ol alcohol (Panel d) and h)). $\chi$ is the molar fraction of the tested vapor in air. The dotted lines are guide for the eye.

the extent of the swelling in the PMMA nanocomposites upon exposure to the different solvent vapors irrespectively of the filler shape. Furthermore a more pronounced response towards all the investigated solvents should be expected for the spherical NC rather than for the NR filler based PMMA composite. In fact, Fig. 5 points out two relevant features that are not fitting with the above expectation, namely i. the swelling extent induced by the polar solvents in PMMA is increased in the presence of spherical NCs, while is reduced by the incorporation of NRs, ii. more extensive swelling is observed in the PMMA filled with the NRs rather than with the spherical NCs, when

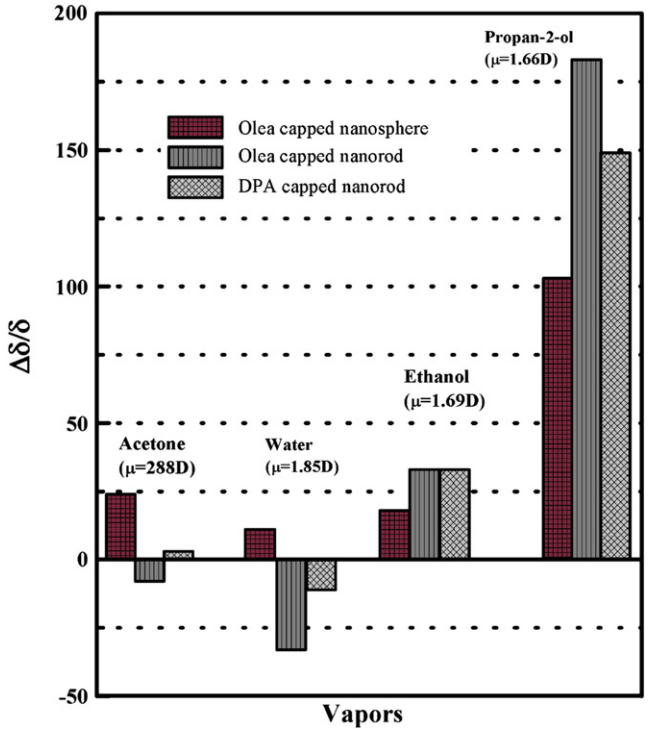


**Fig. 5.** Relative variation of solvent uptake at the equilibrium, defined as $\Delta\delta/\delta = (\delta_{TiO_2/PMMA} - \delta_{PMMA})/\delta_{PMMA}$, for the PMMA composites with OLEA capped nanospheres, OLEA capped NRs, and DPA capped NRs at a fixed content of 4%wt., as a function of the different solvents. μ is the electric dipole moment of the solvent molecule.

exposed to the weakly polar solvent. Such evidences unequivocally indicate that a different amount of voids inside the composite samples cannot alone account for the different solvent absorption ability of the PMMA as a function of the geometry of the nanofillers. In fact the shape of the NC surface combined to its organic capping, i.e. the spatial arrangement of the capping molecules at the NC surface, rather represents the key factor to understand the observed results.

The investigated OLEA capped nanofillers consist of nanosized titania cores terminating with a hydrocarbon periphery, as is illustrated in Scheme 1, since a monolayer of OLEA molecules is coordinated, through their polar functional groups $-CO_2^-$, by means of a bidentate type of bonding to the metal atoms at the oxide surface, as reported in the literature [26,27] and confirmed by the FT-IR measurements.

The sites, where the carboxyl group co-ordinate the metal atoms, together with the free Ti–O sites (not coordinated to any specific group) can be easily approached by the diffusing vapor molecules, due to the radial distribution of the OLEA molecules at the spherical surface of titania particle as sketched in Scheme 2.

Due to their polar character, the carboxyl group and/or the Ti–O sites are more prone to efficiently interact with the solvent polar molecules via a strong dipole–dipole interaction, finally resulting in an increased sorption ability of the polymeric matrix toward acetone and water. In the case of the OLEA and DPA capped NRs, the surface is less accessible for the polar molecules, being the capping molecules more densely packed than in the spherical particles.

The similar, although slightly less effective, response of DPA capped NR based composites with respect to the OLEA capped NR based counterpart could be reasonably ascribed to the specific geometry of the coordinating agents in the latter system. Being the OLEA capped NC surface much more hindered, is far less accessible, to polar solvent

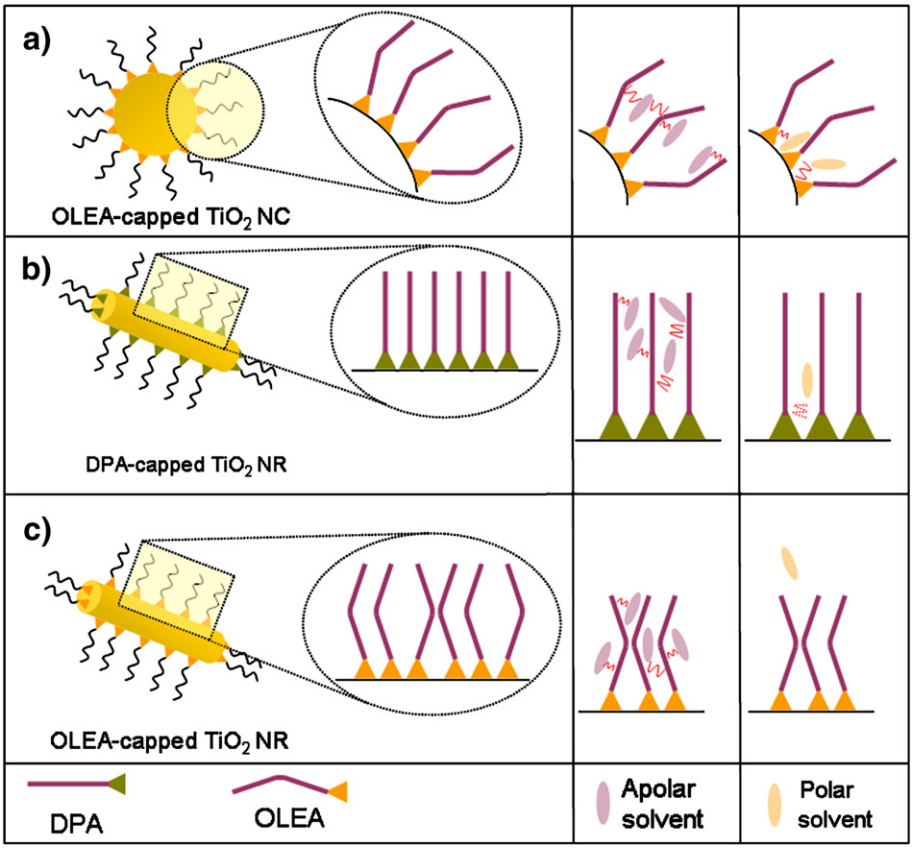


**Scheme 2.** Sketch of the different coordinating molecules at the surface of NCs, as a function of the diverse geometry. In the columns on the right the specific interactions between the capping molecules at NC surface and polar and apolar solvents, respectively, are reported.

molecules, both for the peculiar arrangement of the alkyl chains due to the cis-type conformation, and for the length of the aliphatic moiety (C18 in OLEA vs C12 in DPA) (Scheme 2).

The overall features characterizing the OLEA capping molecules result in a NR surface far more difficult to access for the polar solvent molecules with respect to the case of DPA NRs.

Concomitantly, the occurrence, in the case of the DPA capped NRs, of a polar head group i. e. phosphonate, which is known to involve both tridentate and bidentate binding modes for the coordination to the titania surface [29] plays a role in explaining the slightly higher sensitivity of the DPA capped NR based composites. Namely the presence of a residual P–OH group in the bidentate bonds makes the surface of the nanosized titania more available to polar solvents, hence imparting a weak sensitivity to the polar solvents. At the same time the interaction between the shorter DPA aliphatic chains and the C–H bonds of the weakly polar solvents, causes the reduced absorption capacity observed in the DPA capped NR containing PMMA when exposed to the ethanol and propan-2-ol with respect to the case of the OLEA capped NR based equivalent.

## 4. Conclusions

In this paper the preparation and the characterization of nanocomposite materials based on the incorporation of $TiO_2$ NCs, differing in shape and surface chemistry, in PMMA have been reported. Swelling measurements in the presence of polar and apolar solvent molecules have been performed in order to test the role played by the nanoparticle dispersion in the polymer moiety on the solvent absorption properties of PMMA. The results of the investigation have demonstrated that NC geometry and surface chemistry can modify the specific absorption characteristics of the PMMA and increase the nanocomposite sensitivity to different solvent molecules, namely acetone, ethanol, propan-2-ol and water. Such features, ascribed to specific interactions between the analyte vapors and the organic capped NC surface, can be suitably tailored in a very precise and reliable way and thus have a large impact for designing original and high selective chemical sensors.

## Acknowledgments

The partial support of the Italian MIUR SINERGY programme (FIRB RBNE03S7XZ) and “Nanostructured semiconductors in photocatalytic processes for environmental protection of lapideous material” Strategic Project funded by Regione Puglia (Italy), within the Scientific Research Framework Program 2006. The authors acknowledge B. Antonazzo for the TEM measurements, which have been carried out at the NNL Laboratories in Lecce, Italy.

## References

[1] I. Gorelikov, E. Kumacheva, Chem. Mater. 16 (2004) 4122.
[2] W. Caseri, Macromol. Rapid Commun. 21 (2000) 705.
[3] P. Judeinstein, C. Sanchez, J. Mater. Chem. 6 (1996) 511.
[4] S. Komarneni, J. Mater. Chem. 2 (1992) 1219.
[5] D.Y. Godovski, Adv. Polym. Sci. 119 (1995) 79.
[6] L.L. Beecroft, C.K. Ober, Chem. Mater. 9 (1997) 1302.
[7] A. Convertino, A. Capobianchi, A. Valentini, E.N.M. Cirillo, Adv. Mater. 15 (2003) 1103.
[8] S.T. Selvan, J.P. Spatz, H.A. Klok, M. Moller, Adv. Mater. 10 (1998) 132.
[9] H.J. Chen, P.C. Jian, J.H. Chen, L. Wang, W.Y. Chiu, Ceram. Int. 33 (2007) 643.
[10] L. Pang, Y. Shen, K. Tetz, Y. Fainman, Opt. Express 13 (2005) 44.
[11] C.H. Hung, W.T. Whang, J. Mater. Chem. 15 (2005) 267.
[12] M. Tamborra, M. Striccoli, R. Comparelli, M.L. Curri, A. Petrella, A. Agostiano, Nanotechnology 15 (2004) S240.
[13] M. Tamborra, R. Comparelli, M.L. Curri, M. Striccoli, A. Petrella, A. Agostiano, in: P. Lugli, L.B. Kish, J. Mateos (Eds.), Microtechnologies for the New Millennium, Sevilla, Spain, May 9–11, 2005, SPIE Proceedings, 5838, 2005, p. 236.
[14] M.K. Corbierre, N.S. Cameron, M. Sutton, K. Laaziri, R.B. Lennox, Langmuir 21 (2005) 6063.
[15] I. Potapova, R. Mruk, S. Prehl, R. Zentel, T. Basche, A. Mews, J. Am. Chem. Soc. 125 (2003) 320.
[16] A. Convertino, A. Valentini, A. Bassi, N. Cioffi, L. Torsi, E.N.M. Cirillo, Appl. Phys. Lett. 80 (2002) 1565.
[17] K.P. Gritsenko, A. Capobianchi, A. Convertino, J. Friedrich, R.D. Schulze, V. Ksensov, S. Schrader, in: Satoru Iwamori (Ed.), Kerala, India: Research Signpost, 2005, p. 85.
[18] A. Convertino, G. Leo, M. Striccoli, G. Di Marco, M.L. Curri, Polymer 49 (2008) 5526.
[19] K. Haraguchi, T. Takehisa, Adv. Mater. 14 (2002) 1120.
[20] A. Convertino, G. Leo, M. Tamborra, C. Sciancalepore, M. Striccoli, M.L. Curri, A. Agostiano, Sens. Actuators B Chem. 126 (2007) 138.
[21] T. Vossmeyer, B. Guse, I. Besnard, R.E. Bauer, K. Müllen, A. Yasuda, Adv. Mater. 14 (2002) 238.
[22] R.A. Potyrailo, A.M. Leach, Appl. Phys. Lett. 88 (2006) 134110.
[23] S.D. Evans, S.R. Johnson, Y.L. Cheng, T. Shen, J. Mater. Chem. 10 (2000) 183.
[24] M. Li, Y. Chen, Sens. Actuators B 32 (1996) 83.
[25] P.D. Cozzoli, A. Kornowski, H. Weller, J. Am. Chem. Soc. 125 (2003) 14539.
[26] P.J. Thistlethwaite, M.S. Hook, Langmuir 16 (2000) 4993.
[27] M. Nara, H. Torii, M. Tasumi, J. Phys. Chem. 100 (1996) 19812.
[28] W. Gao, L. Dickinson, C. Grozinger, F.G. Morin, L. Reven, Langmuir 12 (1996) 6429.
[29] G. Guerrero, P.H. Mutin, A. Vioux, Chem. Mater. 13 (2001) 4367.
[30] Y. Ebenstein, E. Nahum, U. Banin, Nano Lett. 2 (2002) 945.
[31] M. Born, E. Wolf, Principles of Optics Pergamon, 1964, New York, 51 pp.
[32] The change in the refractive index of the PMMA matrix caused by the swelling follows from the Lorentz–Lorenz formula (in Ref. [17]). Assuming that the additional volume of the film was due to solvent uptake we have that the refractive index of the swollen film, $n_{tot}$, is $n_{tot} = \{[(n_1^2 \cdot X_1)/(n_1^2+2) + (n_2^2 \cdot X_2)/(n_2^2+2)]/[X_1/(n_1^2+2) + X_2/(n_2^2+2)]\}^{1/2}$ where $X_1$ and $X_2$ are the volume fractions, and $n_1$ and $n_2$ are the bulk refractive indices of the PMMA ($n_1$ ¼ 1.54 from reference sample) and the solvent, in: R.C. Weast (Ed.), Handbook of Chemistry and Physics, CRC Press, 1978–1979., respectively. For example, in the case of the acetone, which is the solvent inducing the highest degree of swelling, taking into account an amount of X2 of 25%, we obtain a variation of the refractive index Δn/n around 1%.
[33] C. Brosseau, F. Boulic, P. Queffelec, C. Bourbigot, Y. Le Mest, J. Loaec, J. Appl. Phys. 81 (1997) 882.
[34] A. Bassi, A. Valentini, A. Convertino, Appl. Phys. A 71 (2000) 109.
[35] N. Cioffi, I. Farella, L. Torsi, A. Valentini, L. Sabbatini, P.G. Zambonin, Sens. Actuators B Chem. 93 (2003) 181.